Canadian Mineralogist
Vol. 22, pp. 347-356 (1984)

EQUILIBRIA IN THE SYSTEM Fe-C-O AND THE ORIGIN OF NATIVE IRON

JERRY R. WEIDNER
Department of Geology, University of Maryland, College Park, Maryland 20742, U.S.A.

ABSTRACT

The equilibrium relationships among the phases iron (I), graphite (G), oxide liquid (Lo), metallic liquid (Lm) and gas (V) in a portion of the system Fe–C–O were experimentally determined at pressures up to 2 kbar. An invariant point located at 1142 ± 5°C and 0.53 ± 0.05 kbar is the origin of the univariant reactions: 1) I + Lo + G = Lm, 2) I + G + V = Lm, 3) Lo + G = Lm + V, 4) Lo + G = I + V and 5) Lo + Lm = I + V. The data indicate that iron carbide, Fe_3C, is metastable with respect to the assemblage graphite + iron at magmatic temperatures and pressures up to 2 kbar. The phase relations show that native iron can result from the ascent of graphite-bearing mafic magma, as proposed by Pedersen (1981) and Bird *et al.* (1981) for the native iron found in the volcanic rocks of Disko Island, Greenland. In the case of the Uivfaq native iron (Bird *et al.* 1981), the phase equilibria suggest that cohenite rims on iron grains and iron oxide liquids were generated by oxidation processes during cooling. Some of the wüstite in the Uivfaq iron probably crystallized from iron oxide liquid at about 850°C.

Keywords: native iron, system Fe–C–O, metallic iron liquid, graphite–gas equilibria, oxidation–reduction, cohenite, iron oxide liquid.

SOMMAIRE

On a déterminé jusqu'à une pression de 2 kbar les relations d'équilibre entre les phases fer natif (I), graphite (G), bain fondu à base d'oxyde (Lo), bain fondu métallique (Lm) et phase gazeuse (V) dans une partie du système Fe–C–O. Un point invariant se trouve à 1142 ± 5°C, 0.53 ± 0.05 kbar; il est à l'origine des réactions univariantes suivantes: 1) I + Lo + G = Lm, 2) I + G + V = Lm, 3) Lo + G = Lm + V, 4) Lo + G = I + V et 5) Lo + Lm = I + V. Les données montrent que le carbure de fer Fe_3C est métastable par rapport à l'assemblage graphite + fer à température magmatique et jusqu'à 2 kbar. Elles indiquent que le fer natif pourrait résulter de l'ascension d'un magma mafique porteur de graphite, comme l'ont proposé Pedersen (1981) et Bird *et al.* (1981) pour le fer natif des roches volcaniques de l'île de Disko (Groënland). Dans le cas du fer natif d'Uivfaq (Bird *et al.* 1981), les données expérimentales font penser que le liseré de cohenite entourant les grains de fer et le bain fondu d'oxyde de fer ont pris naissance par oxydation au refroidissement. Une partie de la wüstite dans la phase métallique d'Uivfaq aurait cristallisé à partie d'un bain fondu d'oxyde à environ 850°C.

(Traduit par la Rédaction)

Mots-clés: fer natif, système Fe–C–O, bain fondu métallique, équilibre graphite - phase gazeuse, oxydation–réduction, cohenite, bain fondu à base d'oxyde.

INTRODUCTION

This note describes the invariant and univariant equilibria in the system Fe–C–O among metallic iron, graphite, vapor, oxide liquid and metallic liquid at magmatic temperatures and pressures up to 2 kbar. An earlier report (Weidner 1982) emphasized the phase relations involving graphite, iron oxides and oxide liquid, and showed that iron oxide liquids were produced between 0.2 and 2 kbar at less than 1000°C. The work reported here is an extension of that study to include metallic liquid and iron.

Interest in graphite–iron equilibria has been recently stimulated by the recognition of graphite in several stratiform igneous complexes, including Skaergaard, Greenland (Sato & Valenza 1980), the Duluth complex, Minnesota (Hollister 1980), Stillwater, Montana and Bushveld, South Africa (Elliott *et al.* 1981) as well as in submarine basaltic glass and mantle-derived peridotite nodules recovered from alkalic basalt (Mathez & Delaney 1981).

The petrogenetic significance of graphite in these rocks stems from the oxidation–reduction properties of graphite–gas equilibria as a function of temperature and especially pressure. The oxygen fugacity $f(O_2)$ of this equilibrium is strongly pressure-dependent; low pressures, less than 1 kbar, produce $f(O_2)$ values in the metallic iron stability-field at magmatic temperatures (French & Eugster 1965). Osborn (1959) showed that the crystallization history of mafic magmas may be significantly affected by the $f(O_2)$ of the system. Sato (1977, 1978) pointed out that basaltic systems containing graphite and gas must become more reducing with decreasing pressure and suggested this mechanism to account for native iron in lunar basalts (Sato *et al.* 1973). Similar mechanisms have been proposed to account for the native iron found in some rocks from Disko, Greenland (Pedersen 1981, Bird *et al.* 1981). The Uivfaq native iron (Disko Island), described in detail by Bird *et al.* (1981), is relevant here because the native iron - wüstite mineral assemblages are similar to those observed in this study. The experimental system provides a model for the interpretation of some features found in these unusual rocks.

EXPERIMENTAL METHODS

The experimental data were obtained by the conventional quench technique wherein known compositions are heated in sealed noble-metal containers at fixed temperatures and pressures for periods of time sufficient for reaction to occur, cooled rapidly to room temperature, and the container contents examined to establish the phases present at the temperature and pressure of the experiment. Additional experiments using differential thermal analysis (DTA) were carried out to test assumptions and interpretations required by the quench method. A detailed description of the apparatus, reagents, and analytical methods are given in Weidner (1982) and are summarized below.

Experiments were made in internally heated, argon-medium pressure vessels (Yoder 1950) equipped with manganin pressure-sensing cells and Inconel-sheathed thermocouples. The experiments at 0.1 kbar were made in cold-seal pressure vessels (Tuttle 1949) using Bourdon tube gauges and Inconel-sheathed thermocouples. The accuracy of temperature measurement is ± 10°C or better. The reported pressure values are accurate to ± 5% or better. Quench experiments were made by pumping argon into the vessel to about 70% of the desired pressure, increasing the temperature to 900°C, making final pressure adjustments, holding the temperature at this value for about 45 minutes, slowly increasing the temperature to the desired value and manually controlling the temperature for one hour. Temperature control, including any overshot, was ± 2°C or less. The initial quench-rate was about 200°C/min.

All experiments were made using graphite crucibles sealed within 2.5-mm-diameter platinum capsules. Total duration of an experiment was about two hours. The short duration and the use of a graphite crucible minimized contamination of the metallic phase by platinum. The platinum content of quenched metallic phases ranged from 0.07 wt.% to less than the detection limit, approximately 0.01 wt.%, and was measured using a Cambridge Microscan-5 electron microprobe. Platinum contamination was judged to be insignificant.

Four compositions, (1) 20%Fe_2O_3–80%C, (2) 20%$FeCO_3$–80%C, (3) 2%Fe_2O_3–18%Fe–80%C, (4) 20%Fe–80%C, in weight percent, were used for most of the quench experiments and were prepared by manually homogenizing reagent-grade materials (see Weidner 1982) in air for about 15 minutes using an agate mortar and pestle. The carbon in the bulk compositions given above includes the graphite crucible as well as graphite mixed with the other reagents. Graphite and vapor were always present in experiments using the first two compositions, whereas a metallic phase and graphite were always present when the last two compositions were used. Vapor-absent experiments using composition (4) always produced final assemblages that contain about 0.5% wüstite. The oxide is due to surface contamination on the iron starting material and air in sealed capsules. In addition, several experiments were made using mixtures of Fe_2O_3 and Fe standardization wire (99.90% pure, 220 μm diameter). The mixtures were weighed directly into the graphite crucible in proportions similar to composition (3) above. This was useful because the original morphology of the wire was destroyed only if melting occurred.

THE PRODUCTS OF THE EXPERIMENTS

The properties and interpretation of experiment products are described in the following section. The properties are those observed in samples heated in the temperature range 1000–1200°C unless otherwise indicated. The analyses were made using binocular stereoscopic and petrographic reflected-light microscopy supplemented where necessary by X-ray powder-diffraction methods.

The hematite–graphite and siderite–graphite starting mixtures were used primarily to locate the reactions oxide liquid + graphite = iron + vapor and oxide liquid + graphite = metallic liquid + vapor (Fig. 1). Both mixtures always included graphite and vapor among the phases present. A vapor phase was indicated by puffed sample-containers and a meniscus on quenched liquids. The quenched charges from experiments at pressures higher than the above reactions always contained a vesiculated aggregate of wüstite with irregular patches and rims of magnetite and usually showed a meniscus. This is typical of the oxide liquid - graphite - vapor assemblage quenched from temperatures above 1000°C (Weidner 1982). The remaining compositions, including the experiments using iron wire, always produced quench assemblages that included metallic phases and graphite. Experiments using these mixtures at pressures higher than the oxide liquid + graphite = iron + vapor and oxide liquid + graphite = metallic liquid + vapor reactions were vapor-absent, as indicated by capsules tightly molded around the charges and the presence of 1-to-50-μm spherical to ameboid masses of wüstite within the metallic aggregate. Weidner (1982) showed that iron oxide liquids are produced from the iron - wüstite - graphite assemblage at about 850°C at comparable pressures. Therefore the wüstite is interpreted as quenched iron oxide liquid. The metallic aggregate, in the range 1000 to 1140°C, typically consists of a single predominantly iron-bearing mass containing, in addition to the wüstite noted above, irregular flakes of graphite and about 15% (visual estimate) of randomly oriented and evenly dispersed cementite Fe_3C needles up to 150 μm in length and 20 μm in width. The original shape of the iron wire was preserved when used in the starting material. Experiments at 1130°C and 2 kbar lasting 48 hours produced identical samples. Because the amount, habit and size of the cementite needles did not change with

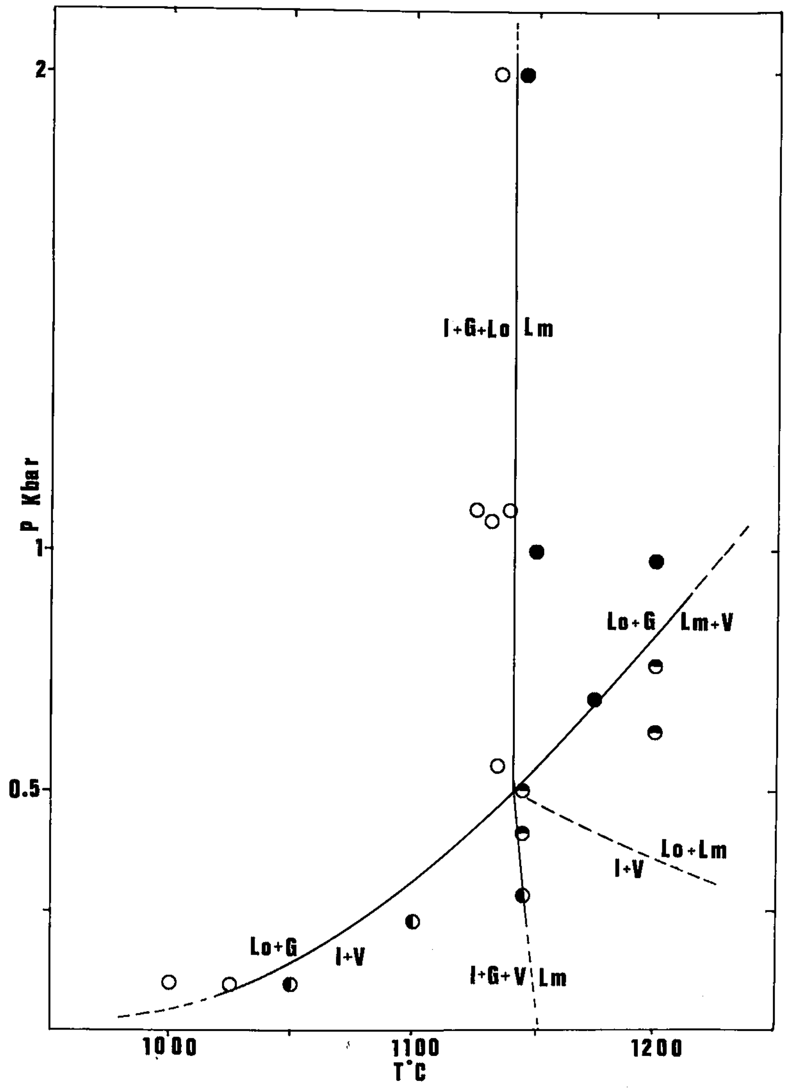

FIG. 1. T–P projection showing the results of experiments locating the invariant point and associated univariant curves. Open circles indicate the assemblages Lo + G + V, I + Lo + G. Left-half-filled circles indicate the assemblage I + G + V. Top-half-filled circles indicate the assemblage Lm + G + V. Filled circles indicate the assemblages Lo + G + V, Lo + Lm + G. Abbreviations: Lo oxide liquid, Lm metallic liquid, I iron, G graphite, V gas.

time, the cementite is interpreted as a metastable phase produced by exsolution from graphite-saturated γ-iron during the quench. Similar textures are observed in hypereutectic iron–carbon alloys heat-treated and quenched at one atmosphere. The solubilities of graphite and cementite in iron are nearly identical and decrease from about 2 wt. % at the eutectic (~1152°C) to about 0.75 wt. % at the eutectoid (~738°C) (Darken & Gurry 1953). Although metastable with respect to graphite, cementite exsolves from the graphite-saturated γ-iron during the quench (see also Reed-Hill 1964). Vapor-absent assemblages heated at 1145°C possess wüstite and graphite similar to the above, and iron wire starting material retained some of its original shape; otherwise, the texture of the metallic aggregate was quite different. The metallic aggregate consisted of approximately equal volumes of iron and cementite. Avout half the aggregate occurs in lens-shaped domains about 300 μm long and 50 μm wide made up of a vermicular intergrowth of iron and optically continuous cementite. The remainder of the typical sample consists of coarse cementite dendrites (~ 100 μm length and 10 μm width) with interstitial iron. This texture is interpreted as quenched metallic liquid. Similar experiments at 1150°C and higher temperatures produced identical textures except that the metal and oxide phases were dispersed throughout the walls of the graphite crucible. No textural features suggesting primary cementite crystals were observed. Note, however, that cementite becomes a stable phase at higher pressure (Ringwood 1960, Hilliard 1963). Korsunskaya *et al.* (1976) indicated that cohenite becomes a stable phase at about 1 kbar and temperatures near the eutectic. Their estimate is based on thermochemical calculation and experiments at 30 and 90 kbar. Experiments at 1000°C and 20 kbar (J. Weidner, unpubl. data) produce assemblages of cementite, wüstite and graphite. No metallic iron is present. The cementite occurs as equant, euhedral, 20-to-40-μm grains and has a texture that is quite different from any described in this report. The experimental data indicate that cementite in equilibrium with graphite and wüstite (or oxide liquid) is not stable in the 1000–1200°C range at pressures up to 2 kbar, but becomes stable at some pressure less than 20 kbar.

When heated at pressures less than necessary for the reactions oxide liquid + graphite = iron + vapor and oxide liquid + graphite = metallic liquid + vapor to occur (Fig. 1), all compositions studied consist of vapor - graphite - metallic liquid assemblages. Usually, no iron oxide phases were observed in the quenched samples. The texture of the quenched metallic phases is identical to that noted above. The only significant difference is shown by metallic liquid, which typically occurs as one or two smooth-surfaced metallic spheres instead of being dispersed in the walls of the graphite crucible. This morphology also confirms the presence of a vapor phase.

TABLE 1. RESULTS OF DTA EXPERIMENTS

Cycle No.	T°C	P kbar	Reaction
1	735	1.38	αI + G = γI
1	997	1.52	I + G + W = Lo
1	1141	1.58	I + G + Lo = Lm
2	740	1.41	αI + G = γI
2	958	1.48	I + G + W = Lo
2	1137	1.48	I + G + Lo = Lm
3	738	1.40	αI + G = γI
3	1008	1.51	I + G + W = Lo
3	1140	1.51	I + G + Lo = Lm
4	738	4.00	αI + G = γI
4	959	4.25	I + G + W = Lo
4	1152	4.41	I + G + Lo = Lm

Abbreviations: I iron, W wüstite, G graphite, Lo oxide liquid, Lm metallic liquid.

The assemblages observed in quench experiments are thought to represent a close approach to equilibrium. Except for cementite in metallic iron, four-phase assemblages were virtually never observed, and experiments having a 48-hour duration produced identical results. This conclusion was tested by carrying out differential thermal analysis (DTA) experiments in the range 700 to 1200°C and 1 to 4 kbar using a 350 mg starting mixture of $18.8\%Fe_2O_3$–$64.5\%Fe$–$16.7\%C$ (wt. %). The instrument was calibrated against the α- to β-quartz transition (Yoder 1950) at pressures up to 4 kbar and NaCl melting (800.5°C) at one atmosphere. After an initial heating cycle to 1200°C, the starting mixture is vapor-absent and consists of wüstite, graphite, α-iron and cementite. The results of a representative DTA experiment, consisting of four heating cycles, are shown in Table 1. Each cycle consists of (1) cooling from 1200 to 700°C at about 200°C/min., (2) a 0.5 hr. stabilization period at 700°C and (3) heating at about 80°C/min. to 1200°C. During heating, three endothermic effects are observed. The highest-temperature event is very strong and sharp and corresponds with the reaction iron + graphite + oxide liquid = metallic liquid, with a precision of ± 3°C on both the heating and cooling cycles. The lowest-temperature effect is very sharp, but low in amplitude, and agrees closely with the eutectoid α-iron + graphite = γ-iron reaction at 738 ± 3°C (Wells 1938). It is also reproducible to ± 3°C on both heating and cooling. The close agreement between heating and cooling is unexpected because the metastable formation of cementite is enhanced by rapid cooling and the metastable eutectoid reaction α-iron + cementite = γ-iron (723°C) (Hansen & Anderko 1958) is usually observed in metallurgical studies at one atmosphere (*e.g.*, Reed-Hill 1964). The samples used here differ from a typical metallurgical alloy as they contain relatively large quantities of iron oxide and graphite as well as being held at higher pressure. The amplitude of the thermal effect of the peritectic reaction was constant from cycle to cycle, indicating that the content of metallic iron was constant also. All of the observations regarding the peritectic reaction are consistent with the interpretation of cementite as a metastable phase produced during quenching, but would not be expected if cementite were a stable phase. A third, broad, low-amplitude thermal effect is usually observed during heating, but during cooling it is often obscured by the very strong signal and subsequent instability of the recording instrument, produced by the crystallization of the metallic liquid. The third thermal effect represents the oxide-melting reaction iron + graphite + wüstite = oxide liquid. The heating-cycle values are 100 to 150°C higher than the 850°C ± 30°C value reported by Weidner (1982) for pressure between 0.5 and 2 kbar and do not have

TABLE 2. RESULTS OF DEFINITIVE EXPERIMENTS

Run No.	Composition	T°C	P kbar	Results
0496	20Fe:80C	1125	1.17	I + G + tr Lo
0495	"	1132	1.13	I + G + tr Lo
0490	"	1140	1.17	I + G + tr Lo
0489	"	1150	1.00	Lm + G + tr Lo
0493	"	1145	2.00	Lm + G + tr Lo
0494	$2Fe_2O_3$:18Fe:80C	1135	2.00	I + G + Lo
0509	" "	1135	0.55	I + G + Lo
0504	" "	1145	0.50	Lm + G + V
0503	" "	1145	0.41	Lm + G + V
0505	" "	1145	0.28	I + G + V + tr Lm
0491	$20Fe_2O_3$:80C	1200	0.98	Lo + G + V
0492	"	1200	0.76	Lm + G + V
0508	"	1100	0.24	I + G + V
1491	"	1050	0.10	I + G + V
1485	"	1025	0.10	Lo + G + V
1488	"	1000	0.10	Lo + G + V
0501	$20FeCO_3$:80C	1175	0.69	Lo + G + V + tr Lm
0513	" "	1200	0.62	Lm + G + V
1490	" "	1050	0.10	I + G + V
1484	" "	1025	0.10	Lo + G + V
1486	" "	1000	0.10	Lo + G + V

Abbreviations used are: I iron, G graphite, V vapor, Lo oxide liquid, Lm metallic liquid, tr trace amount.
The results indicate the assemblage stable at the conditions of the experiment. The Composition column shows the weight percent of the reagent used in the starting mixture.

high precision. The low precision and accuracy are due to a combination of factors, including the relatively small amount of oxide liquid generated, the rate of melting compared to heating rate and the difficulty in unambiguously defining the temperature at the beginning of the thermal effect. The values reported should be regarded as qualitative only. However, they show that the rate of formation of oxide liquid is rapid relative to the length of the quench experiments made in this study.

Taken together, the observations noted above indicate that equilibrium was closely approached during the quench experiments and that the nature and location of the invariant and univariant equilibria (Fig. 1) are probably correct.

RESULTS AND DISCUSSION

The results of definitive experiments are listed in Table 2 and are shown, in P–T projection, in Figure 1. The location of the univariant reactions was determined according to the reaction criteria described in the preceding section and is also shown in Figure 1. The character of the univariant reactions was derived from the experimental data using the methods of Schreinemachers (1915-1925). The data are sufficient to define and locate an invariant point at 1142 ± 5°C and 0.53 ± 0.05 kbar and the following associated univariant reactions:

iron + oxide liquid + graphite = metallic liquid (1)
iron + graphite + vapor = metallic liquid (2)
oxide liquid + graphite = metallic liquid + vapor (3)
oxide liquid + graphite = iron + vapor (4)
oxide liquid + metallic liquid = iron + vapor (5)

Reactions (1) and (2) are located with a precision of ± 4°C and were used to locate the invariant point by a short extrapolation. The first reaction lies in the vapor-absent region and is vertical within experimental error at pressures up to 2 kbar. The second reaction has a slightly negative slope and passes through 1152°C at one atmosphere (Hansen & Anderko 1958). Reaction (4) is located at 1036 ± 12°C at 100 bars and terminates at 850 ± 30°C (Weidner 1982) and 11 bars (calculated pressure) at an invariant point among the phases iron, oxide liquid, wüstite, graphite and vapor. The pressure of this invariant point was estimated using the equation of French & Eugster (1965), iron–wüstite $f(O_2)$ data (Eugster & Wones 1962), free-energy data for graphite–gas equilibria (Deines *et al.* 1974) and iron-activity data for graphite-saturated iron (Smith 1946, Darken & Gurry 1953). At 1036 ± 12°C and 100 bars, reaction (4) is about 125 bars lower than the value reported by Weidner (1982). The reported pressure of experiment 0500 (Weidner 1982) is incorrect. The graphite-absent reaction, (5), was not experimentally located and its position is only constrained to lie between reaction (2) and the metastable extension of reaction (4). It passes through the point 1524°C (Darken & Gurry 1946) at one atmosphere as the reaction iron + oxide liquid + vapor = metallic liquid, indicating that a singular point exists at some intermediate temperature where the composition of the metallic liquid becomes colinear with iron and vapor. The relation between the univariant and invariant equilibria reported here and the lower-temperature reactions involving iron oxide liquids (Weidner 1982) is shown in the schematic T–P projection (Fig. 2).

Divariant equilibria at 100 bars, shown in Figure 3 as an $f(O_2)$–T projection, illustrate the general relationships among phases existing between about 11 and 300 bars. Divariant equilibria were not measured directly, but rather were derived from the univariant reactions together with available thermochemical data. The isobarically invariant assemblages graphite – vapor – iron – oxide liquid (~1035°C) and graphite – vapor – iron – metallic liquid (~1150°C) are taken from this study, whereas wüstite – graphite – iron – oxide liquid (~850°C) and graphite – vapor – wüstite – oxide liquid (~830°C) are extrapolated from Weidner (1982) (see Fig. 2). Graphite–vapor equilibria are taken from French & Eugster (1965) and include the assemblages graphite – vapor – magnetite, graphite – vapor – wüstite, graphite – vapor – oxide liquid, graphite – vapor – iron and graphite – vapor– metallic liquid. Equilibria involving magnetite – wüstite and wüstite – iron were estimated from the appropriate $f(O_2)$ buffer reactions (Eugster & Wones 1962). The isobarically univariant assemblages iron – oxide liquid – vapor and wüstite – graphite – oxide liquid are each common to two isobarically invariant points and both have undetermined curvature. The iron– graphite –

metallic liquid curve has a slightly negative slope and terminates at about 1152°C (Hansen & Anderko 1958) as the metallic liquid composition approaches the iron–carbon boundary. The remaining equilibria are constructed to be consistent with the topology of the system, but are otherwise schematic. These include the isobarically invariant point magnetite - wüstite - oxide liquid - vapor and associated univariant assemblages wüstite - oxide liquid - vapor and magnetite - oxide liquid - vapor as well as iron - oxide liquid - vapor and iron - metallic liquid - vapor. The quartz - fayalite - iron (QFI) $f(O_2)$ buffer (Eugster & Wones 1962) is included for comparison.

The phase relations shown in Figures 1, 2 and 3 provide a useful model for considering the origin of native iron, wüstite and related minerals presumed to have been produced by reactions between graphite and mafic magma. The general oxidation–reduction properties of graphite–gas equilibria have been discussed by many investigators (*e.g.*, French & Eugster 1965, Eugster & Skippen 1967, Ohmoto & Kerrick 1977, Frost 1979). The implication of graphite in igneous rocks has been considered by Sato & Valenza (1980) and Mathez & Delaney (1981). For purposes of discussion, the effect of graphite will be considered as two separate mechanisms: 1) reduction during isothermal decompression and 2) oxida-

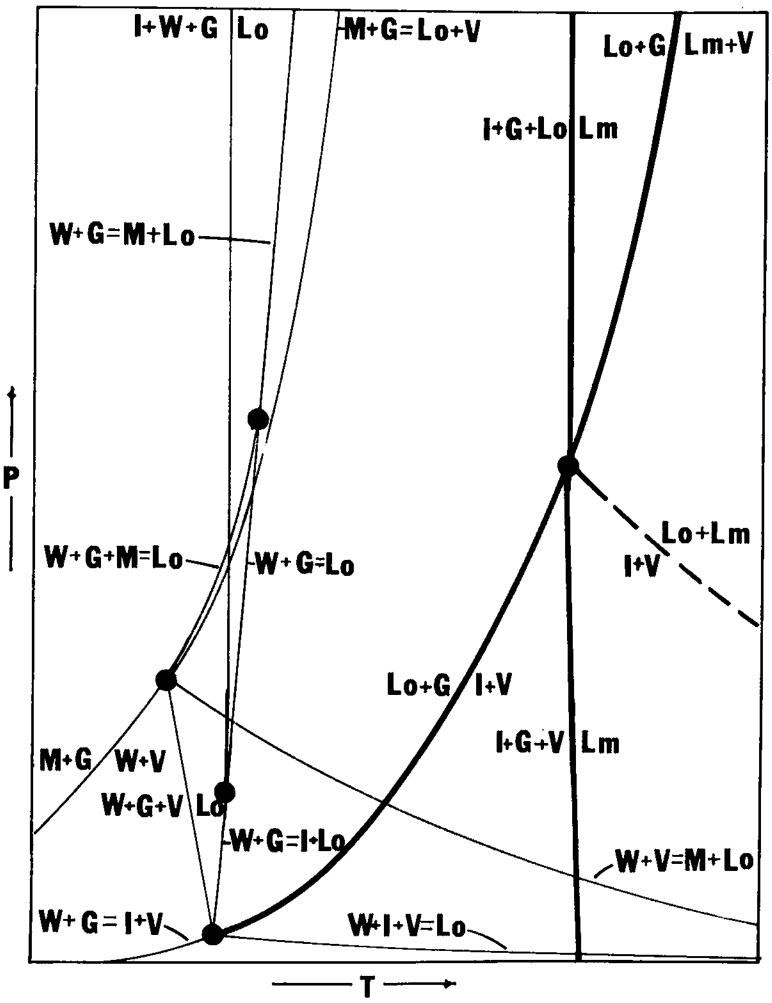

FIG. 2. Schematic T-P projection showing the relation between the results of this study (heavy lines) and the univariant and invariant equilibria involving the formation of oxide liquids (Weidner 1982). Abbreviations: M magnetite, W wüstite, Lo oxide liquid, Lm metallic liquid, I iron, G graphite, V gas.

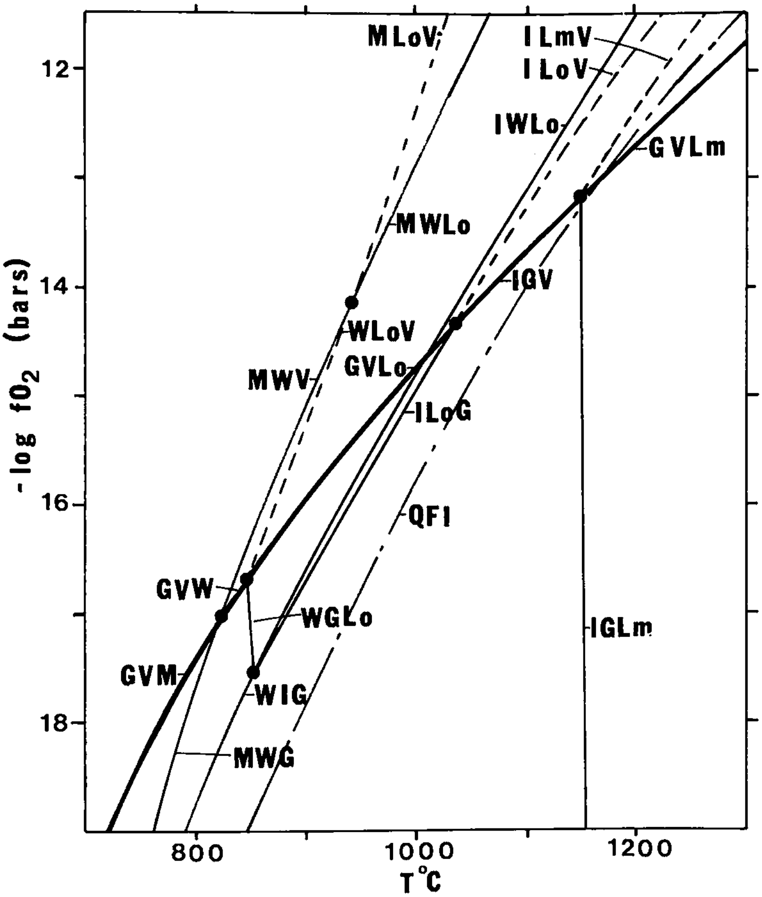

FIG. 3. T-$f(O_2)$ projection showing univariant and divariant equilibria at 100 bars. The heavy line defines graphite–gas equilibria. QFI is the quartz–fayalite–iron $f(O_2)$ buffer (Eugster & Wones 1962). Abbreviations: M magnetite, W wüstite, Lo oxide liquid, Lm metallic liquid, I iron, G graphite, V gas.

tion during isobaric cooling. The simplifying assumptions of a pure C–O gas phase and equilibrium also are made.

Reduction during isothermal decompression

Reduction during isothermal decompression arises from the fact that the $f(O_2)$ of graphite–gas equilibria is much more sensitive to a pressure change than the $f(O_2)$ of reactions involving condensed phases such as the standard $f(O_2)$ buffers (Eugster & Wones 1962) or crystal–liquid equilibria in basaltic magma (Haggerty 1976). For example, the isothermal decompression of a graphite–gas system at 1100°C from 2 kbar to 100 bars results in a decrease in $f(O_2)$ of about two orders of magnitude (French & Eugster 1965), whereas the $f(O_2)$ of condensed reactions is virtually unchanged (Huebner 1971). Consequently, the isothermal ascent of a mafic magma saturated in graphite + gas must cause reduction, as pointed out by Sato & Valenza (1980), and may produce metallic iron at shallow levels, as observed in many Disko Island rocks (Bird *et al.* 1981, Pedersen 1981). The decompression–reduction process only functions if both graphite and gas are present. If the graphite is consumed or the system is vapor-absent, *i.e.*, the $f(O_2)$ of the system is different from the $f(O_2)$ of the graphite–gas equilibrium, then reactions involving condensed phases govern the $f(O_2)$, and graphite (or gas) has no particular effect on oxidation–reduction processes. In the system Fe–C–O, the reactions oxide liquid + graphite = iron + vapor and oxide liquid + graphite = metallic liquid + vapor (Fig. 1) define the P–T conditions at which metallic iron could be produced by the isothermal decompression of assemblages containing graphite + vapor. These reactions probably have no direct natural analogues because the activity of other components, *e.g.*, silica and titania, is too high in most natural systems. The intersection of the graphite + vapor surface and the QFI $f(O_2)$ buffer (Fig. 3) provides a more reasonable estimate of the conditions necessary to generate metallic iron phases by isothermal decompression in natural systems. A pressure of 100 bars is about the upper limit at which a pure or nearly pure metallic iron phase could be produced at 1150 to 1200°C. Most natural magmatic systems would probably require somewhat lower pressures.

Oxidation during isobaric cooling

In contrast to the effect of decreasing pressure, isobaric cooling of assemblages containing graphite + gas causes oxidation in the system Fe–C–O and probably has a similar effect in natural magmas. This conclusion stems from the fact that the slope of the isobaric $f(O_2)$–T surface for graphite + gas is significantly less than that of the condensed phase $f(O_2)$ buffers and natural mafic systems (Haggerty 1976). Compare, for example, the slopes of the graphite - vapor - iron, graphite - vapor - oxide liquid and graphite - vapor - wüstite surfaces with graphite - iron - oxide liquid, graphite - wüstite - iron and the QFI $f(O_2)$ buffer (Fig. 3). The graphite–vapor equilibria culminate in the oxidation of wüstite to magnetite, whereas the vapor-absent reactions involving condensed phases remain strongly reducing. The oxidation of natural systems would tend to behave in a similar fashion. In general, the slope of the $f(O_2)$–T surface of natural condensed phase-assemblages is similar to the vapor-absent curves shown in Figure 3 (Haggerty 1976). Natural systems would probably produce ferrous silicates as the principal product of oxidation rather than iron oxide liquids, unless the silica activity were unusually low.

Application to natural assemblages

The assemblages native iron - armalcolite - iron-poor pyroxene found in graphite-bearing volcanic rocks (Disko) were probably produced by the decompression–reduction mechanism (Pedersen 1981). Pedersen noted that these rocks are the most highly reduced terrestrial rocks reported and suggested that the reduction process stopped because the graphite was nearly consumed. The phase relations in Figure 3 indicate that the reduction process will also stop once the gas pressure becomes equal to the lithostatic pressure. Preservation of the reduced assemblage during cooling requires that the vapor phase be lost from the system, *i.e.*, the assemblages be vapor-absent and the $f(O_2)$ be buffered by the crystalline aggregate rather than graphite–gas reactions.

The native Uivfaq iron described by Bird *et al.* (1981) appears to be an example of decompression–reduction followed by oxidation upon isobaric cooling. This is indicated by the inclusion of fayalite, ferriferous pigeonite, wüstite, magnetite, FeO-rich glass and other phases within blocks of massive iron and iron carbide. This assemblage is significantly more oxidized than the native-iron-bearing rocks described by Pedersen (1981). The presence of wüstite indicates that oxidation has taken place and that a vapor phase was present during cooling. Bird *et al.* (1981) suggested that some of the wüstite crystallized in equilibrium with carbon-saturated iron at temperatures above 1100°C. The results of this study indicate that primary wüstite formed at much lower temperatures, probably about 850°C, from an iron oxide liquid.

Some of the cohenite found in the Uivfaq iron may also be a product of the mechanism of oxidation during isobaric cooling. Bird *et al.* (1981) reported cohenite rims on grains of iron as well as the occurrence of cohenite in several other morphologies. Cohenite is the natural analogue of the cementite observed in this study and is metastable with respect to graphite. As pointed out by Bird *et al.* (1981), nucleation kinetics favor the precipitation of cohenite instead of graphite. The presence of wüstite in these assemblages indicates that oxidation did occur and a vapor phase was present. If this is true, then several reactions leading to carbon precipitation probably occurred during the cooling of the Uivfaq iron. The exsolution of cohenite from carbon-saturated γ-iron and the metastable γ-iron = α-iron + Fe_3C eutectoid reaction account for some of the habits of cohenite (Bird *et al.* 1981). In addition to simple carbon-exsolution reactions from iron–carbon alloys, three additional carbon-producing mechanisms probably occurred, and each would tend to form a cohenite rim-structure on grains of carbon-saturated iron: (a) The isobaric cooling of a C–O gas phase in equilibrium with graphite (or cohenite) precipitates carbon according to the reaction $2CO = CO_2 + C$. (b) During the oxidation of iron, some metallic iron must be consumed, and the carbon content of the remaining iron must increase. If the iron is carbon-saturated, then the carbon would be precipitated. (c) Similarly, the removal of oxygen from the gas phase during oxidation of iron must increase the carbon content of the gas, and, if the gas is in equilibrium with graphite (or cohenite), carbon would be precipitated. If nucleation kinetics favor cohenite over graphite, then a rim of cohenite would be expected on the surface of the iron grain where the reactions are occurring. Note that the oxidation referred to here is not necessarily a late-stage deuteric process. Figure 3 indicates that the assemblage iron

– graphite – vapor would oxidize to oxide liquid – graphite – vapor at 1035°C and 100 bars. The oxide liquid so generated would crystallize to wüstite at about 830°C provided both graphite and vapor are present during cooling.

The discussion and conclusions presented in the preceding paragraph are generalizations drawn from the relationships in the simple system Fe–C–O. Their application to natural systems require the usual caveats. If the analogous phases in the natural systems are relatively pure, say 95 percent or greater, then the conclusions reached here are probably valid. As to the question of the presence of other species in the vapor phase, many basaltic systems can reasonably be assumed to be virtually anhydrous. If so, hydrogen and methane would be minor diluents and would not significantly change the phase equilibria discussed in this report. A similar conclusion is reached for sulfur. Pedersen (1981) indicated that reactions involving sulfides had no discernable effect on the graphite oxidation–reduction process in the native-iron- and graphite-bearing rocks he described.

ACKNOWLEDGEMENTS

The experimental work described here was carried out in the experimental petrology laboratories at Stanford University, Goddard Space Flight Center and at the University of Maryland. Financial support was provided by the National Science Foundation and the National Aeronautic and Space Administration. The comments of the referees were most helpful. Special thanks are due C. Goodrich for a copy of her recent dissertation (Cornell University) describing the petrogenesis of Disko Island iron–carbon alloys and for drawing my attention to the work of Korsunskaya *et al.* (1975).

REFERENCES

BIRD, J.M., GOODRICH, C.A. & WEATHERS, M.S. (1981): Petrogenesis of Uivfaq iron, Disko Island, Greenland. *J. Geophys. Res.* **86**, 11787-11805.

DARKEN, L.S. & GURRY, R.W. (1946): The system iron–oxygen. II. Equilibrium and the thermodynamics of liquid oxide and other phases. *J. Amer. Chem. Soc.* **68**, 798-816.

______ & ______ (1953): *Physical Chemistry of Metals.* McGraw-Hill, New York.

DEINES, P., NAFZIGER, R.H., ULMER, G.C. & WOERMANN, E. (1974): Temperature–oxygen fugacity tables for selected gas mixtures in the system C–H–O at one atmosphere total pressure. *Earth Mineral Sci. Expt. Station. The Pennsylvania State University, University Park. Pa. Bull.* **88.**

ELLIOTT, W.C., ULMER, G.C., GRANDSTAFF, D.E. & GOLD, D.P. (1981): A graphite-platinum association in layered intrusives? *Amer. Geophys. Union Trans.* **62**, 421 (abstr.).

EUGSTER, H.P. & SKIPPEN, G.B. (1967): Igneous and metamorphic reactions involving gas equilibria. *In* Researches in Geochemistry 2 (P.H. Abelson, ed.). John Wiley & Sons, New York.

______ & WONES, D.R. (1962): Stability relations of the ferruginous biotite, annite. *J. Petrology* **3**, 82-125.

FRENCH, B.M. & EUGSTER, H.P. (1965): Experimental control of oxygen fugacities by graphite–gas equilibriums. *J. Geophys. Res.* **70**, 1529-1539.

FROST, B.R. (1979): Mineral equilibria involving mixed-volatiles in a C–O–H fluid phase: the stabilities of graphite and siderite. *Amer. J. Sci.* **279**, 1033-1059.

HANSEN, M. & ANDERKO, K. (1958): *Constitution of Binary Alloys.* McGraw-Hill, New York.

HAGGERTY, S.E. (1976): Opaque mineral oxides in terrestrial igneous rocks. *In* Oxide Minerals (D. Rumble III, ed.). *Mineral. Soc. Amer. Rev. Mineral.* **3**, Hg 101-300.

HILLIARD, J.E. (1963): Iron–carbon phase diagram: isobaric sections of the eutectoid region at 35, 50, and 65 kilobars. *Trans. Metall. Soc. A.I.M.E.* **227**, 429-438.

HOLLISTER, V.F. (1980): Origin of graphite in the Duluth complex. *Econ. Geol.* **75**, 764-766.

HUEBNER, J.S. (1971): Buffering techniques for hydrostatic systems at elevated pressures. *In* Research Techniques for High Pressure and High Temperature (G.C. Ulmer, ed.). Springer-Verlag, New York.

KORSUNSKAYA, I.A., KAMENETSKAYA, D.S. & ERSHOVA, T.P. (1976): Phase equilibriums in the iron–carbon system at high pressures and high temperatures. *High Temperatures — High Pressures* **8**, 661-662.

MATHEZ, E.A. & DELANEY, J.R. (1981): The nature and distribution of carbon in submarine basalts and peridotite nodules. *Earth Planet. Sci. Lett.* **56**, 217-232.

OHMOTO, H. & KERRICK, D. (1977): Devolatilization equilibria in graphic systems. *Amer. J. Sci.* **277**, 1013-1044.

OSBORN, E.F. (1959): Role of oxygen pressure in the crystallization and differentiation of basaltic magma. *Amer. J. Sci.* **257**, 609-647.

PEDERSEN, A.K. (1981): Armalcolite-bearing Fe–Ti oxide assemblages in graphite-equilibrated salic volcanic rocks with native iron from Disko, central west Greenland. *Contr. Mineral. Petrology* **77**, 307-324.

REED-HILL, R.E. (1964): *Physical Metallurgy Principles*. D. van Nostrand, Princeton, New Jersey.

RINGWOOD, A.E. (1960): Cohenite as a pressure indicator in iron meteorites. *Geochim. Cosmochim. Acta* **20**, 155-158.

SATO, M. (1977): The driving mechanism of lunar pyroclastic eruptions inferred from the oxygen fugacity behavior of Apollo 17 orange glass. *Amer. Geophys. Union Trans.* **58**, 425 (abstr.).

______ (1978): Oxygen fugacity of basaltic magmas and the role of gas-forming elements. *Geophys. Res. Lett.* **5**, 447-449.

______ (1979): The driving mechanism of lunar pyroclastic eruptions inferred from the oxygen fugacity behavior of Apollo 17 orange glass. *Proc. Lunar Planet. Sci. Conf.* **10**, 311-325.

______, HICKLING, N.L. & MCLANE, J.E. (1973): Oxygen fugacity values of Apollo 12, 14 and 15 lunar samples and reduced states of lunar magmas. *Proc. Lunar Sci. Conf.* **4**, 1061-1064.

______ & VALENZA, M. (1980): Oxygen fugacities of the layered series of the Skaergaard intrusion, east Greenland. *Amer. J. Sci.* **280-A**, 134-158.

SCHREINEMAKERS, F.A.H. (1915-1925): In-, mono- and divariant equilibria. *Koninkl. Akad. Wetenschappen te Amsterdam*. Collection of papers reprinted (1965) by The Pennsylvania State University, University Park, Pa.

SMITH, R.P. (1946): Equilibrium of iron–carbon alloys with mixtures of CO–CO_2 and CH_4–H_2. *J. Amer. Chem. Soc.* **68**, 1163-1175.

TUTTLE, O.F. (1949): Two pressure vessels for silicate–water studies. *Geol. Soc. Amer. Bull.* **60**, 1727-1729.

WEIDNER, J.R. (1982): Iron-oxide magmas in the system Fe–C–O. *Can. Mineral.* **20**, 555-566.

WELLS, C. (1938): Graphitization in high purity iron–carbon alloys. *Amer. Soc. Metals Trans.* **26**, 289-357.

YODER, H.S., JR. (1950): The high-low quartz inversion up to 10,000 bars. *Amer. Geophys. Union Trans.* **31**, 827-835.

Received April 7, 1983, revised manuscript accepted August 12, 1983.